

## Variation of $T_c$ and transport properties with carrier concentration in Y- and Pb-doped Bi-based superconductors

P. Mandal, A. Poddar, and B. Ghosh

*Saha Institute of Nuclear Physics, 92 Acharya Prafulla Chandra Road, Calcutta 700 009, India*

P. Choudhury

*Central Glass and Ceramic Research Institute, 196 Raja Subodh Chandra Mullick Road, Calcutta 700 032, India*

(Received 1 October 1990; revised manuscript received 8 January 1991)

Electrical resistivity, magnetic susceptibility, and the Hall voltage of  $\text{Bi}_2\text{Sr}_2\text{Ca}_{1-x}\text{Y}_x\text{Cu}_2\text{O}_{8+y}$  (Bi 2:2:1:2) and  $(\text{Bi}_{1-x}\text{Pb}_x)_2\text{Sr}_2\text{Ca}_2\text{Cu}_3\text{O}_{10+y}$  (Bi 2:2:2:3) samples are measured as a function of temperature. A metal-insulator transition originating from the change of carrier concentration is found in the Bi 2:2:1:2 system at  $x \simeq 0.55$ . Analysis of the electrical resistivity in the insulating region suggests that the transport is governed by a variable-range-hopping mechanism in the low-temperature region and phonon-assisted hopping of polarons in the high-temperature region. A universal dome-shaped  $T_c$  versus  $n_H$  variation is observed in the Bi 2:2:1:2 and Bi 2:2:2:3 systems, which is similar to that reported in  $\text{La}_{2-x}\text{Sr}_x\text{CuO}_4$  and  $\text{YBa}_2\text{Cu}_3\text{O}_{7-x}$  systems. Various normal-state parameters, such as the effective mass of the carrier, Fermi energy, density of states at the Fermi level, and correlation energy, are calculated and compared to those reported in the literature.

### I. INTRODUCTION

The well-established phase diagram of the  $\text{CuO}_2$ -based superconductors is that the systems are Mott-Hubbard insulating in the low-carrier-concentration region and superconducting in the intermediate range, whereas in the heavily doped region they are normal metals.<sup>1-5</sup> The carrier concentration in the high- $T_c$  systems may be varied by varying the dopant and oxygen contents. Ong *et al.*<sup>6</sup> observed a linear relation between the carrier concentration ( $n_H = 1/R_H e$ ,  $R_H$  is the Hall constant) and the doping concentration ( $x$ ) in the  $\text{La}_{2-x}\text{Sr}_x\text{CuO}_4$  (2:1:4) system. The superconducting transition temperature ( $T_c$ ) is strongly related to  $n_H$  in the 2:1:4 (Ref. 2) and  $\text{YBa}_2\text{Cu}_3\text{O}_{7-x}$  (1:2:3) (Refs. 4 and 5) systems.  $T_c$  increases with the increase of the carrier concentration, passes through a maximum, and then decreases and becomes zero beyond a critical concentration. For the superconducting samples,  $R_H$  is strongly temperature dependent,  $R_H^{-1}$  being linear in  $T$ . However, for low carrier concentration,  $R_H$  is, in general, temperature independent.<sup>4,5,7</sup> The concentration at which maximum  $T_c$  is observed varies from system to system. The values are 0.15 (Ref. 2), 0.25, (0.5 in a single crystal) (Ref. 6), 0.25–0.35 (Refs. 8 and 9), 0.20 (Refs. 10 and 11), and 0.10–0.15 (Ref. 12) per Cu ion for the 2:1:4, 1:2:3,  $\text{Bi}_2\text{Sr}_2\text{Ca}_{1-x}\text{Y}_x\text{Cu}_2\text{O}_{8+y}$  (Bi 2:2:1:2),  $(\text{Bi}_{1-x}\text{Pb}_x)_2\text{Sr}_2\text{Ca}_2\text{Cu}_3\text{O}_{10+y}$  (Bi 2:2:2:3), and  $\text{Tl}_2\text{Ba}_2\text{Ca}_2\text{Cu}_3\text{O}_{10+y}$  (Tl 2:2:2:3) systems, respectively. Uemura *et al.*<sup>13</sup> from muon-spin relaxation studies, observed a universal linear relation between  $T_c$  and  $n_s/m^*$  for the four high- $T_c$  systems where  $n_s$  is the superconducting carrier density and  $m^*$  is the effective mass. They also found saturation and suppression of  $T_c$  in the heavily doped samples. Moreover, saturation starts at

different levels of  $n_s/m^*$  and increases progressively in 2:1:4, 1:2:3, 2:2:1:2, and 2:2:2:3 systems. A similar relation between  $T_c$  and  $\omega_p^2$  ( $\omega_p$  is the plasma frequency) was observed by Tanaka<sup>14</sup> from an optical measurement.

Most of the reports available on the resistivity and Hall coefficient of the high- $T_c$  systems are in that region of carrier concentration where the systems are superconducting. Comparatively less amount of work has been done in the nonsuperconducting concentration. Studies in this region are also useful in understanding the mechanism of superconductivity. In the 2:1:4 system, transport properties in this region have been studied by several workers.<sup>15,16</sup> Ellman *et al.*<sup>16</sup> measured the resistivity ( $\rho$ ) of  $\text{La}_{2-x}\text{Sr}_x\text{CuO}_4$  ( $0.02 \leq x \leq 0.10$ ) samples near the metal-insulator (MI) transition point. In the low-temperature region ( $T \leq 8$  K),  $\rho(T)$  follows a relation

$$\rho = \rho_0 \exp[(T_0/T)^n], \quad (1)$$

where  $\rho_0$ ,  $T_0$ , and  $n$  are constants. For the  $x = 0.02$  sample, a best fit of  $\rho(T)$  is obtained for  $n = \frac{1}{2}$  and  $T_0 = 74$  K, whereas for  $x = 0.05$  these values are  $\frac{1}{4}$  and 645 K.  $n = \frac{1}{4}$  is indicative of a Mott variable-range-hopping (VRH) mechanism in three dimensions.<sup>17</sup> The localization length ( $\alpha^{-1}$ ) calculated from  $T_0$  is large (16–30 Å), suggesting that the system is near the MI transition point. Matsuda *et al.*<sup>4</sup> made similar analysis on  $\text{Y}_{1-x}\text{Pr}_x\text{Ba}_2\text{Cu}_3\text{O}_{7-y}$  for  $x > 0.7$  where the system becomes insulating. The observed resistivity is neither a three-dimensional (3D) VRH ( $n = \frac{1}{4}$ ) nor an activation ( $n = 1$ ) type. In the oxygen-deficient  $\text{EuBa}_2\text{Cu}_3\text{O}_{7-x}$  sample, a 2D VRH ( $n = \frac{1}{3}$ ) is observed in the temperature range 14–125 K (Ref. 18). In the Bi 2:2:1:2 system, Tamegai *et al.*<sup>8</sup> obtained  $n = \frac{1}{3}$  (2D VRH) while Yoshizaki *et al.*<sup>19</sup> obtained  $n = \frac{1}{4}$  (3D VRH) in a limited tem-

perature range.

In the present work we have studied the electrical resistivity, magnetization, and Hall effect of  $\text{Bi}_2\text{Sr}_2\text{Ca}_{1-x}\text{Y}_x\text{Cu}_2\text{O}_{8+y}$  and  $(\text{Bi}_{1-x}\text{Pb}_x)_2\text{Sr}_2\text{Ca}_2\text{Cu}_3\text{O}_{10+y}$  samples. The  $T_c$  versus  $n_H$  plot in these systems also follows a universal dome-shaped curve as found in the 2:1:4 and 1:2:3 systems.<sup>2,4</sup> Moreover,  $n_H$  is linear with the Y concentration ( $x$ ) in  $\text{Bi}_2\text{Sr}_2\text{Ca}_{1-x}\text{Y}_x\text{Cu}_2\text{O}_{8+y}$ , the behavior predicted for a strongly correlated Mott-Hubbard system.<sup>20</sup> For  $\text{Bi}_2\text{Sr}_2\text{Ca}_{1-x}\text{Y}_x\text{Cu}_2\text{O}_{8+y}$  ( $x > 0.55$ ), the resistivity is insulating in nature and, in the low-temperature region, the transport property is governed by a 2D VRH mechanism ( $n = \frac{1}{3}$ ). At  $x = 0.55$ ,  $n$  changes from  $\frac{1}{3}$  to  $\frac{1}{4}$ , indicating a crossover from a 2D VRH to a 3D VRH mechanism. In the high-temperature region ( $T \geq \Theta_D/2$ ,  $\Theta_D = \text{Debye temperature} \approx 300 \text{ K}$  for high- $T_c$  systems<sup>21</sup>), the best fit of  $\rho(T)$  yields  $n = 1$  for  $x > 0.55$ . Thus, the resistivity in the high-temperature region is thermally activated. The thermally activated resistivity and temperature independent  $R_H$  (for  $x > 0.45$ ) predict an activated mobility in this system which suggests that the transport in this region may be due to hopping of polarons.

## II. SAMPLE PREPARATION

$\text{Bi}_2\text{Sr}_2\text{Ca}_{1-x}\text{Y}_x\text{Cu}_2\text{O}_{8+y}$  ( $x = 0-1.0$ ) samples with different nominal compositions were prepared by mixing powders of  $\text{Bi}_2\text{O}_3$ ,  $\text{SrCO}_3$ ,  $\text{CaCO}_3$ ,  $\text{Y}_2\text{O}_3$ , and  $\text{CuO}$  (all 99.999% pure) in the appropriate ratio and calcinating at  $850^\circ\text{C}$  for 24 h in air. The product was recalculated several times in air with intermediate grindings for a total span of firing time more than 90 h. The recalcination temperature ( $860^\circ\text{C}$  for  $x = 0$  and  $900^\circ\text{C}$  for  $x = 1.0$ ) was increased linearly with the doping concentration ( $x$ ). Finally, the product was ground, pressed into pellets and annealed in air at the above-mentioned temperature for more than 48 h. We have also prepared one  $\text{Bi}_2\text{Sr}_2\text{Ca}_1\text{Cu}_2\text{O}_{8+y}$  sample by the matrix method. In this case,  $\text{SrCO}_3$ ,  $\text{CaCO}_3$ , and  $\text{CuO}$  powders were mixed in the ratio 2:1:2 and fired at  $960^\circ\text{C}$  for a few days with intermediate grindings. Powders of  $\text{Bi}_2\text{O}_3$  and  $\text{Sr}_2\text{CaCu}_2\text{O}_5$  were then mixed in the ratio 1:1, pressed into pellets, fired at  $930^\circ\text{C}$  for 1 h, and quenched to room temperature. This procedure was repeated for a second time and then annealed in air at  $850^\circ\text{C}$  for more than 12 h. (To distinguish the two  $\text{Bi}_2\text{Sr}_2\text{CaCu}_2\text{O}_{8+y}$  samples, one was prepared directly and the other by the matrix method; hereafter, the former sample is referred to as sample *A* and the latter as sample *B*.)  $(\text{Bi}_{1-x}\text{Pb}_x)_2\text{Sr}_2\text{Ca}_2\text{Cu}_3\text{O}_{10+y}$  ( $x = 0.125-0.3$ ) samples were prepared by mixing powders of  $\text{Bi}_2\text{O}_3$ ,  $\text{PbO}$ ,  $\text{SrCO}_3$ ,  $\text{CaCO}_3$ , and  $\text{CuO}$  in the appropriate ratio and calcinating twice at  $850^\circ\text{C}$  in air for 48 h with intermediate grinding. The product was ground, pressed into pellets, and annealed at  $860^\circ\text{C}$  for a prolonged time (150 h) to increase the volume fraction of the high- $T_c$  phase.

## III. EXPERIMENT

The samples were characterized by the powder x-ray-diffraction method using  $\text{Cu K}\alpha$  radiation. The resistivi-

ty of the samples was measured by the standard dc four-probe technique. For the semiconducting samples ( $x > 0.5$ ), a very small current (1–100  $\mu\text{A}$ ) was used to avoid any Joule heating which might change the sample temperature. For the Hall voltage measurement low-resistance contacts to the sample [ $10.0 \times 3.0 \times (0.15-0.30) \text{ mm}^3$ ] were made by applying a conductive silver paint in the desired configuration and annealing at  $400^\circ\text{C}$  for about 30 min. A Keithley 181 nanovoltmeter was used for resistivity and Hall voltage measurements. The magnetic field ( $B$ ) applied for the Hall voltage measurements was 20 kOe and the current ( $I$ ) was 30 mA. For proper alignment, the sample was rotated about an axis parallel to the current direction until the Hall voltage became maximum and was kept fixed in this position. At each temperature, for a particular value of  $I$  and  $B$ , 8–10 sets of independent measurements were made and their average was used to calculate the Hall coefficient  $R_H$ . Hall voltage measurements were performed in the temperature range where the magnetoresistance of the samples is negligible.

## IV. RESULTS AND DISCUSSION

### A. X-ray analysis

The x-ray-diffraction patterns show that all the  $\text{Bi}_2\text{Sr}_2\text{Ca}_{1-x}\text{Y}_x\text{Cu}_2\text{O}_{8+y}$  samples are single phase having orthorhombic structure. The lattice parameters  $a$  and  $c$  for the  $\text{Bi}_2\text{Sr}_2\text{Ca}_{1-x}\text{Y}_x\text{Cu}_2\text{O}_{8+y}$  ( $x = 0-0.7$ ) samples are plotted in Fig. 1 against the yttrium concentration ( $x$ ). As  $x$  increases, the  $c$  parameter decreases gradually while the  $a$  parameter shows an increase. An analysis of our data indicates orthorhombic distortion with  $b$  slightly larger than  $a$  in all the samples. The presence of small orthorhombicity has also been observed in  $\text{Bi}_2\text{Sr}_2\text{Ca}_1\text{Cu}_2\text{O}_{8+y}$  single crystals.<sup>22</sup> The lattice parameters obtained in the present work are in good agreement with those reported earlier.<sup>8</sup> The decrease of  $c$ -axis

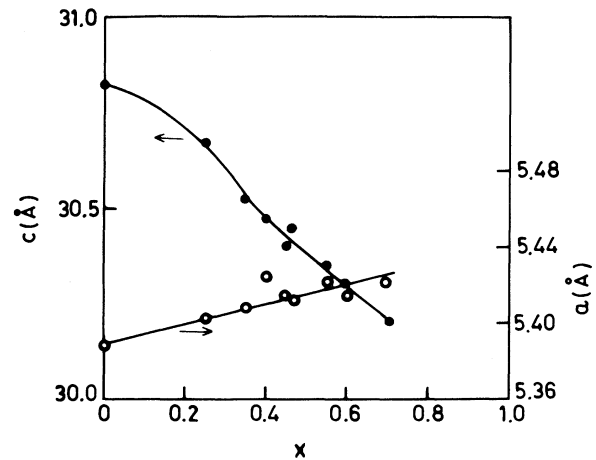


FIG. 1. The variation of the lattice parameters  $a$  and  $c$  with  $x$  in the  $\text{Bi}_2\text{Sr}_2\text{Ca}_{1-x}\text{Y}_x\text{Cu}_2\text{O}_{8+y}$  samples.

length with increasing  $x$  is due to the smaller size of the  $Y^{3+}$  ion compared to the  $Ca^{2+}$  ion. However, it is very difficult to understand the increase in the  $a$  parameter from the substitutional point of view since the  $a$ -axis length is controlled by the in-plane Cu—O bond distance. The increase in  $a$  may be due to the decrease of hole concentration that weakens the Cu—O bonding. As the carrier concentration decreases, the number of  $Cu^{3+}$  ions, which form a shorter Cu—O bond length compared to the  $Cu^{2+}$  ions, decreases. A similar variation in the  $a$  and  $c$  parameters has also been observed in the La system when the  $La^{3+}$  ion is replaced by a slightly larger  $Sr^{2+}$  ions.<sup>23</sup>  $(Bi_{1-x}Pb_x)_2Sr_2Ca_2Cu_3O_{10+y}$  ( $x < 0.25$ ) samples contain a major amount of the 2:2:2:3 phase ( $c = 37.1 \text{ \AA}$ ) and a small amount of the 2:2:1:2 phase ( $c = 30.7 \text{ \AA}$ ). Both of the phases are orthorhombic in structure. For  $x \geq 0.25$  the 2:2:1:2 phase dominates in the sample. Details of the x-ray analysis for some of the  $(Bi_{1-x}Pb_x)_2Sr_2Ca_2Cu_3O_{10+y}$  samples are reported elsewhere.<sup>24</sup>

### B. Resistivity

The temperature dependence of the resistivity for the  $Bi_2Sr_2Ca_{1-x}Y_xCu_2O_{8+y}$  ( $x = 0-0.7$ ) system is shown in Figs. 2(a) and 2(b). For comparison, the resistivity for sample *B* is also shown in the figure. The transition temperature ( $T_c^{R=0}$ ) of this sample is 81 K, which is 15 K higher than that of sample *A* prepared by a direct solid-state reaction. Figure 2 shows that  $T_c^{R=0}$  decreases gradually with the increase of yttrium concentration ( $x$ ). Samples with  $x \leq 0.5$  are superconducting and show metallic behavior in the normal state. As the Y content is increased beyond 0.5, the resistivity shows a change from metallic behavior [ $\rho = \rho_0 + aT$ ] to a semiconducting behavior, particularly in the low-temperature region. For instance, the  $x = 0.55$  sample shows a metallic behavior at high temperature ( $T > 130 \text{ K}$ ) and a semiconducting behavior in the low-temperature region ( $T < 130 \text{ K}$ ). These two regions are separated by a shallow minimum ( $\rho_{\min}$ ) at about 130 K ( $T_{\min}$ ). For other samples ( $x > 0.55$ ),  $\rho_{\min}$  has not been observed in the measured temperature range (20–300 K). The appearance of  $\rho_{\min}$  has been detected in other systems also, e.g., at  $x \leq 0.065$  in the  $La_{2-x}Sr_xCuO_4$  (Ref. 16) and  $x \geq 0.47$  in  $EuBa_2Cu_3O_{7-x}$  (Ref. 18) samples. The absence of minimum in the  $\rho$  versus  $T$  curve in our samples with  $x > 0.55$  suggests that  $\rho_{\min}$  in these samples occurs at a relatively higher temperature ( $> 300 \text{ K}$ ).

The semiconducting behavior in the  $\rho$  versus  $T$  curve below  $T_{\min}$  follows Eq. (1). The value of the exponent  $n$  determines the nature of the conduction mechanism in the semiconducting region of the sample. Data of the insulating samples<sup>25</sup> are analyzed using Eq. (1) with a least-squares fit between 20 to 300 K. The results are presented in Figs. 3(a)–3(c). Below 140 K, the resistivity of all the insulating samples ( $x = 0.60-1.0$ ) may be well described by relation (1) with  $n = \frac{1}{3}$ . This suggests that the conduction in the low-temperature region is governed by a two-dimensional variable-range-hopping mechanism.<sup>26</sup> For  $x = 0.55$ , the best fit is, however, obtained with  $n = \frac{1}{4}$

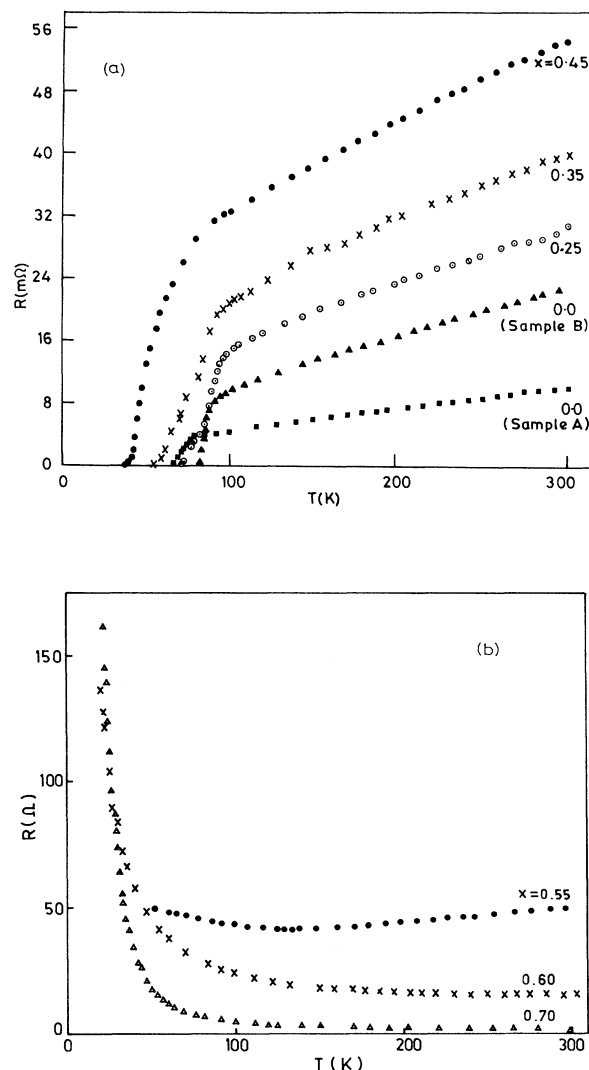


FIG. 2. (a) The temperature dependence of the resistance for the  $Bi_2Sr_2Ca_{1-x}Y_xCu_2O_{8+y}$  ( $x = 0-0.45$ ) samples. (b) The temperature dependence of the resistance for the  $Bi_2Sr_2Ca_{1-x}Y_xCu_2O_{8+y}$  ( $x = 0.55-0.70$ ) samples. As the yttrium content in the samples decreases, and to accommodate all of the results in the same graph, the resistance of different samples is multiplied with suitable factors.

(Ref. 27). Tamegai *et al.*<sup>8</sup> observed a 2D VRH mechanism ( $n = \frac{1}{3}$ ) in  $Bi_2Sr_2Ca_{1-x}Y_xCu_2O_{8+y}$ , whereas Yoshizaki *et al.*<sup>19</sup> reported a three-dimensional VRH ( $n \sim \frac{1}{4}$ ) mechanism for the same system. Our measurement suggests that, for  $x > 0.55$  the conduction at low temperature is governed by a 2D VRH mechanism whereas, for  $x = 0.55$ , a crossover from 2D VRH to 3D VRH occurs.

From the least-squares fit,  $T_0$  for different samples is calculated, which decreases rapidly with the decrease of the Y content. The variation of  $T_0$  as a function of  $1-x$  is presented in Fig. 4. The localization length  $\alpha^{-1}$  ( $\alpha$  is the coefficient of exponential decay of localized states) is

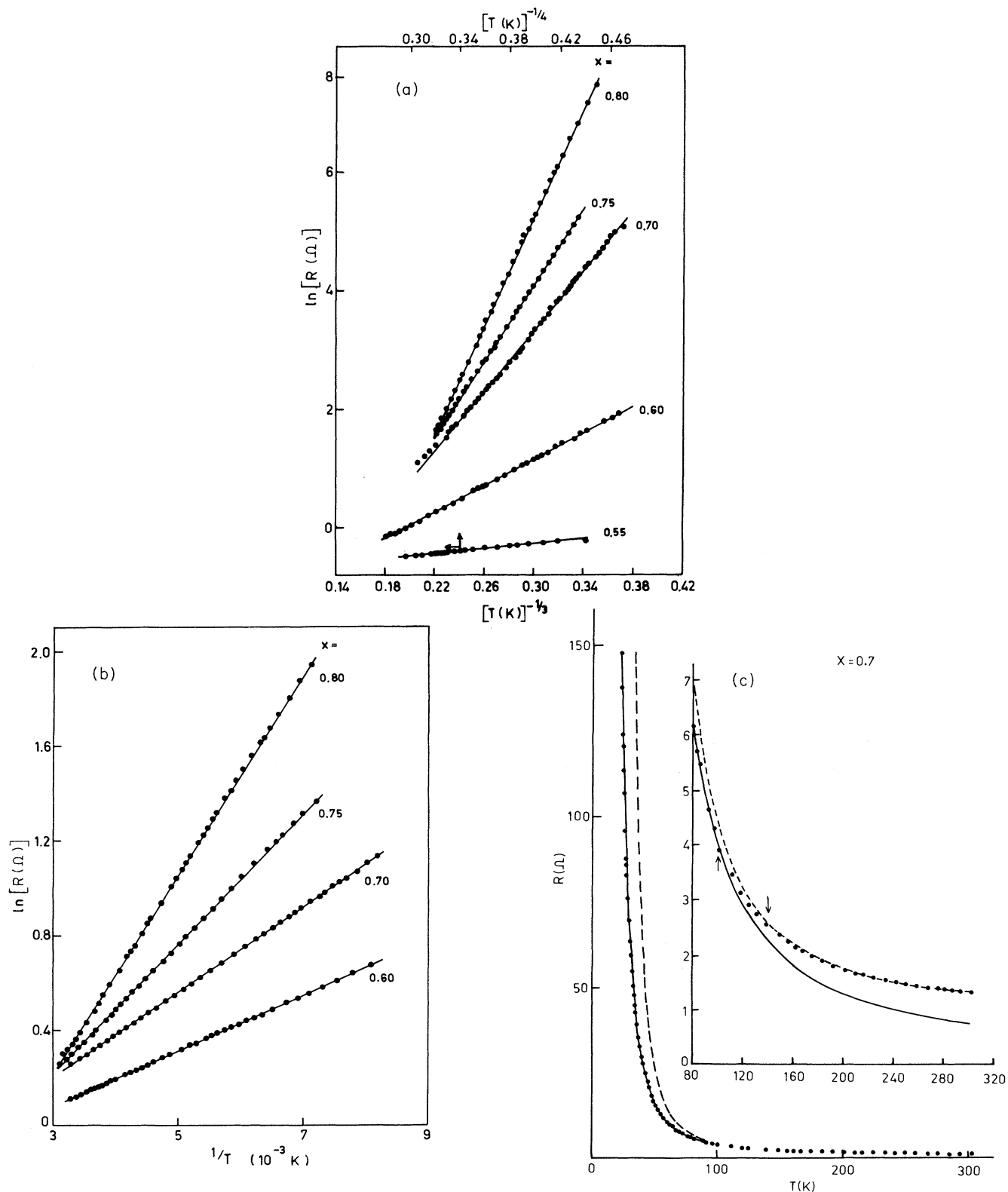


FIG. 3. (a) The logarithm of the low-temperature ( $T < 140$  K) resistance of the  $\text{Bi}_2\text{Sr}_2\text{Ca}_{1-x}\text{Y}_x\text{Cu}_2\text{O}_{8+y}$  samples as a function of  $T^{-1/3}$  for  $x = 0.60$ – $0.80$  (lower scale) and  $T^{-1/4}$  for  $x = 0.55$  (upper scale). (b) The logarithm of the high-temperature ( $T > 140$  K) resistance of the  $\text{Bi}_2\text{Sr}_2\text{Ca}_{1-x}\text{Y}_x\text{Cu}_2\text{O}_{8+y}$  ( $x = 0.60$ – $0.80$ ) samples as a function of  $T^{-1}$ . (c) The temperature dependence of the resistance for the  $\text{Bi}_2\text{Sr}_2\text{Ca}_{1-x}\text{Y}_x\text{Cu}_2\text{O}_{8+y}$  ( $x = 0.70$ ) sample. The solid curve corresponds to the  $\exp[(T_0/T)^{1/3}]$  fit, the dashed curve corresponds to the  $\exp(T_i/T)$  fit, and the solid circles are the experimental points. The high-temperature region has been shown enlarged in the inset.

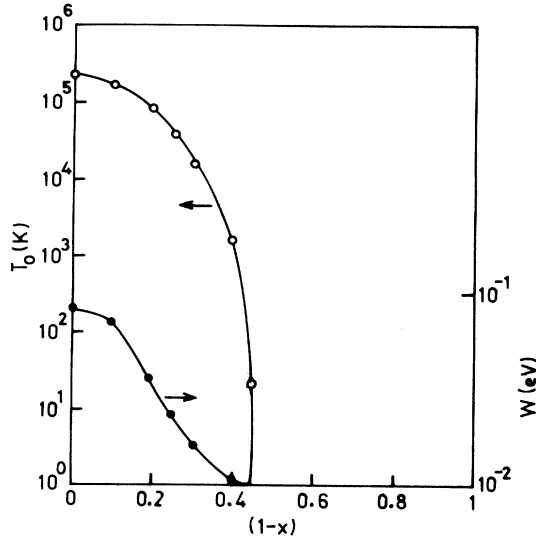


FIG. 4. The variation of  $T_0$  and  $W$  (defined in the text) as a function of  $1-x$  in the  $\text{Bi}_2\text{Sr}_2\text{Ca}_{1-x}\text{Y}_x\text{Cu}_2\text{O}_{8+y}$  samples.

calculated for different samples from the following expression for  $T_0$ :

$$T_0 = \frac{27\alpha^2}{4\pi k_B N(E_F)} \quad \text{for two dimensions} \quad (2a)$$

$$= \frac{16\alpha^3}{k_B N(E_F)} \quad \text{for three dimensions} \quad (2b)$$

(Refs. 28 and 17, respectively), where  $N(E_F)$  is the density of states at the Fermi level and  $k_B$  is the Boltzmann constant. The value of  $N(E_F)$  derived from different measurements<sup>29,30</sup> lies in the range 10–25 states/eV cell, which corresponds to 0.18–0.43 states/eV/Å<sup>2</sup> of the  $\text{CuO}_2$  plane (for two dimensions) and 2.25–5.62  $\times 10^{-2}$  states/eV/Å<sup>3</sup> (for three dimensions). Using these values of  $N(E_F)$ , we estimated the localization length  $\alpha^{-1}$ . For  $x=0.6$ ,  $\alpha^{-1}$  lies in the range 6–10 Å and decreases slowly with the increase in  $x$ . This value of localization length  $\alpha^{-1}$  is approximately 3–5 times the Cu—O bond length in the  $\text{CuO}_2$  plane. At  $x=0.55$ , the system is close to the metal-insulator transition point [ $\alpha^{-1}=60$ –80 Å, as calculated from Eq. (2b)]. As the MI transition is approached,  $T_0$  decreases. The disappearance of  $T_0$  at the transition point may be due to the divergence of localization length. [An increase in  $N(E_F)$  may, however, also lead to a reduction in  $T_0$ .] The nonlocalization of states at a Fermi level below  $x=0.55$  is also evident from the metallic behavior of  $\rho(T)$ . The MI transition at  $x=0.55$  is also seen from the variation of  $\rho_{300}$  with  $x$  (Fig. 5). For low  $x$ , the resistivity is small and increases sharply beyond  $x=0.55$ . A similar MI transition was observed by Clayhold *et al.*<sup>31</sup> in  $\text{Bi}_4\text{Sr}_3\text{Ca}_{3-x}\text{Tm}_x\text{Cu}_4\text{O}_{16+y}$  samples at  $x=1.4$ .

The high-temperature resistivity of  $\text{Bi}_2\text{Sr}_2\text{Ca}_{1-x}\text{Y}_x\text{Cu}_2\text{O}_{8+y}$  ( $x \geq 0.60$ ) fits well with the expression

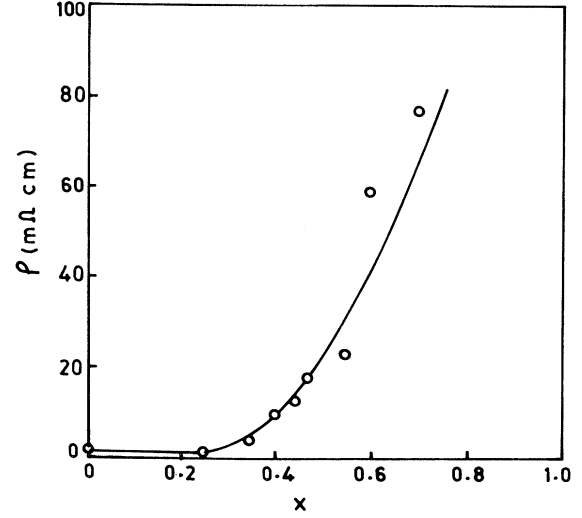


FIG. 5. The variation of the room-temperature resistivity with  $x$  for the  $\text{Bi}_2\text{Sr}_2\text{Ca}_{1-x}\text{Y}_x\text{Cu}_2\text{O}_{8+y}$  samples.

$$\rho = a \exp[T_i/T]^n, \quad n \sim 1, \quad (3)$$

where  $a$  and  $T_i$  are constants. This suggests that the conduction in high temperature is thermally activated. In Fig. 3(c) we have shown how the resistivity for the  $x=0.70$  sample changes from  $\exp(T_i/T)$  at high temperatures ( $T \geq 150$  K) to  $\exp[(T_0/T)^{1/3}]$  at low temperatures ( $T \leq 100$  K). The Hall coefficient of  $\text{Bi}_2\text{Sr}_2\text{Ca}_{1-x}\text{Y}_x\text{Cu}_2\text{O}_{8+y}$  insulators is almost independent of temperature<sup>8</sup> (see also, Fig. 7). Hence, the mobility ( $\mu = \sigma R_H$ ) has the same temperature dependence as that of the conductivity. The thermally activated mobility is a signature of conduction by polarons.<sup>17</sup> Evidence of the formation of polarons (around the charge carriers) in the high- $T_c$  systems has also been obtained from photoinduced absorption studies.<sup>32</sup>

In case of impurity conduction where both the hopping and disorder take part in the conduction mechanism, the total activation energy ( $W = kT_i$ ) is given by<sup>17</sup>

$$\begin{aligned} W &= W_H + W_D/2 \quad \text{for } T > \Theta_D/2 \\ &= W_D \quad \text{for } T < \Theta_D/4, \end{aligned} \quad (4)$$

where  $W_H$  is the hopping energy of the polaron,  $W_D$  is the disorder energy arising from the energy difference of the neighboring sites due to disorder. Since the Debye temperature ( $\Theta_D$ ) for this system is  $\sim 300$  K (Ref. 21), we may consider that the data points above 140 K correspond to the high-temperature region ( $T \geq \Theta_D/2$ ).

Assuming the high-temperature activation energy  $W$  to be close to the hopping energy  $W_H$  (Ref. 17), one can have a rough estimate of the electron-phonon coupling strength  $\gamma = W_P/k_B\Theta_D$ , where  $W_P$  is the polaron binding energy and equal to  $2W_H$  in the narrow band limit. In the high- $T_c$  oxide systems, it is established that the bandwidth is very narrow for small hole (carrier) concentrations and increases exponentially with the carrier con-

centration.<sup>33</sup> In the  $\text{Bi}_2\text{Sr}_2\text{Ca}_{1-x}\text{Y}_x\text{Cu}_2\text{O}_{8+y}$  system, the large- $x$  region corresponds to the low hole concentration. Tamegai *et al.*<sup>8</sup> found that, for  $x=0.9$ , the carrier concentration is as low as  $3 \times 10^{-3}$  per Cu ion. Assuming that the bandwidth is negligible for such low hole concentrations, we have calculated the value of the electron-phonon coupling strength for  $x=0.9$  as  $\gamma=5.4$ . Such a large value of  $\gamma$  indicates that the electron-phonon interaction is very strong and the corresponding polarons should be small polarons.

To get an idea about the size of the polaron, one can use the formula<sup>17</sup>

$$r_p = \pi \hbar / (2W_p m^*)^{1/2}. \quad (5)$$

For a small bandwidth,  $W_p/2 \cong W_H \cong W$ . From the experimental value of  $W$  ( $\sim 930$  K for  $x=1.0$ ) and  $m^*$  ( $\sim 4m_e$ , see Sec. IV D), the radius of the polaron is estimated to be  $\sim 7$  Å. The activation energy  $W$  decreases sharply with decreasing  $x$  (increasing carrier concentration) for  $x < 0.9$  (Fig. 4). The bandwidth in the high- $T_c$  system increases sharply with carrier concentration;<sup>33</sup> thus, the decrease in  $W$  may be mainly due to the increase in the bandwidth for large carrier concentrations. A reduction in the polaron binding energy also lowers the value of  $W$ .

### C. Magnetic susceptibility

The dc magnetic susceptibility was measured using a vibrating sample magnetometer in a field of 20 kOe. The normal-state susceptibility for different Y-content samples is shown in Fig. 6. Figure 6 shows that  $d\chi/dT$  is negative in the high-temperature region for all the samples we studied. The susceptibility at room temperature decreases with the increase of Y concentration. The appearance of a broad maximum with increasing Y content may be attributed to the short-range 2D antiferromagnetic correlation in the  $\text{CuO}_2$  planes. This behavior of  $\chi(T)$  is very similar to that observed in the  $\text{La}_{2-x}\text{Sr}_x\text{CuO}_{4-y}$  and  $\text{YBa}_2\text{Cu}_3\text{O}_{7-x}$  systems.<sup>34</sup> At high temperature (300 K), if we ignore the very weak Curie-like contribution due to the local moment and subtract the core diamagnetic contribution ( $-2.06 \times 10^{-4}$  emu/mol), the remaining paramagnetic contribution is found to be  $3.8 \times 10^{-4}$  (for  $x=0$ ) to  $2.5 \times 10^{-4}$  emu/mol (for  $x=0.35$ ). If we assume that this component comes from the Pauli paramagnetism and Landau diamagnetism, the Pauli susceptibility is calculated to be  $(5.7-3.7) \times 10^{-4}$  emu/mol.

### D. Hall voltage

The Hall coefficient ( $R_H$ ) of the Bi samples is positive and temperature dependent,  $R_H^{-1}$  being linear in temperature. The temperature dependence of  $R_H^{-1}$  for  $\text{Bi}_2\text{Sr}_2\text{Ca}_{1-x}\text{Y}_x\text{Cu}_2\text{O}_{8+y}$  samples is presented in Fig. 7. The temperature dependence of  $R_H^{-1}$  is weaker in these samples compared to the 1:2:3 system<sup>35</sup> and decreases with the increase of Y concentration. The ratio of  $R_H^{-1}$  at 300 and 120 K for  $x=0$  and 0.45 samples are 1.45 and 1.30, respectively.  $R_H^{-1}$  for samples with  $x > 0.45$  is in-

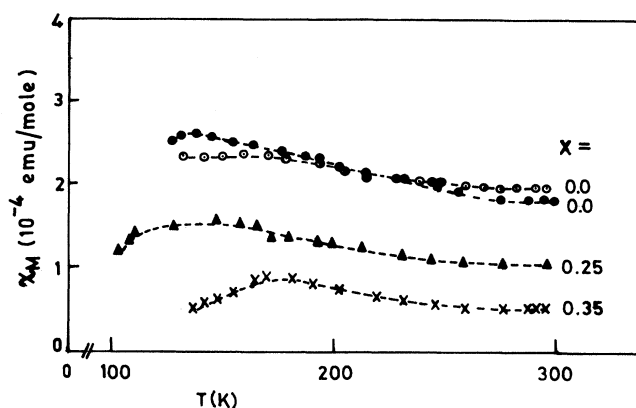


FIG. 6. The temperature dependence of the dc magnetic susceptibility for the  $\text{Bi}_2\text{Sr}_2\text{Ca}_{1-x}\text{Y}_x\text{Cu}_2\text{O}_{8+y}$  ( $x=0-0.35$ ) samples.  $\circ$ : sample A,  $\bullet$ : sample B.

dependent of temperature. The carrier density in these samples is calculated using a single-band model ( $n_H = 1/R_H e$ ). The value of  $n_H$  for sample B ( $x=0$ ) is  $3.1 \times 10^{21} \text{ cm}^{-3}$  and this is in agreement with the value ( $3.0 \times 10^{21} \text{ cm}^{-3}$ ) reported for single crystals.<sup>36</sup> The variation of hole concentration (normalized to formula unit) at 120 K with Y concentration is shown in Fig. 8. The solid line represents the variation of the carrier concentration calculated assuming each Y atom removes one itinerant hole from the  $\text{Bi}_2\text{Sr}_2\text{Ca}_1\text{Cu}_2\text{O}_{8+y}$  system. In this case we assume that the oxygen content of the system is  $\sim 8.30$  so that the system becomes insulating for  $x=0.6$ . Fukuyama and Hasegawa<sup>20</sup> calculated the carrier density for a strongly correlated Hubbard system.

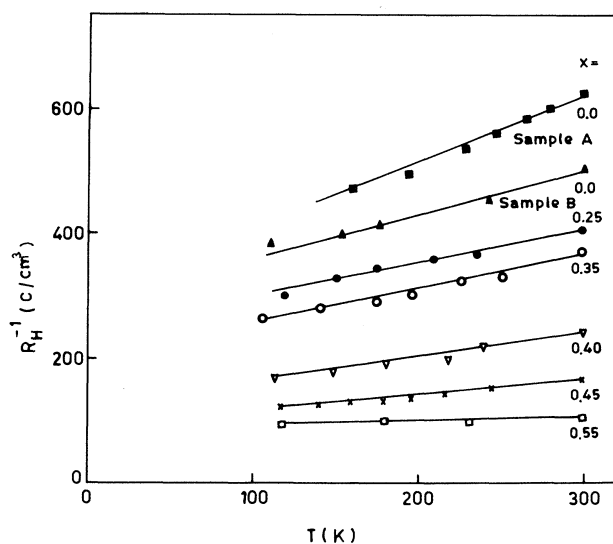


FIG. 7. The variation of the inverse Hall coefficient ( $R_H^{-1}$ ) as a function of temperature for the  $\text{Bi}_2\text{Sr}_2\text{Ca}_{1-x}\text{Y}_x\text{Cu}_2\text{O}_{8+y}$  ( $x=0-0.55$ ) samples.

Their result shows that the Hall coefficient is positive and  $R_H^{-1}$  is proportional to the doping concentration ( $x$ ) for small hole concentration. Figure 8 shows that the measured Hall carrier agrees well with the value calculated by Fukuyama and Hasegawa for strongly correlated systems.

Hall voltage measurements have also been performed in the Pb-doped Bi 2:2:2:3 system. The temperature dependence of  $R_H^{-1}$  for the 2:2:2:3 phase  $(\text{Bi}_{1-x}\text{Pb}_x)_2\text{Sr}_2\text{Ca}_2\text{Cu}_3\text{O}_{10+y}$  samples is plotted in Fig. 9. The temperature dependence of  $R_H^{-1}$  for the 2:2:2:3 system is quite strong and the carrier density is low. The ratio of  $R_H^{-1}$  at 300 and 140 K lies between 2.0 (for  $x=0.15$ ) to 1.6 (for  $x=0.175$ ) (cf. 1.45–1.30 for the 2:2:1:2 system).  $T_c^{R=0}$  is maximum (107 K) for the  $x=0.15$  and minimum (93 K) for the  $x=0.175$  samples and their carrier densities at 300 K are  $2 \times 10^{21}$  and  $3 \times 10^{21} \text{ cm}^{-3}$ , respectively. Rateau *et al.*<sup>10</sup> and Oto *et al.*<sup>11</sup> measured the Hall voltage for the Bi 2:2:1:2 and 2:2:2:3 systems and they also observed a strong temperature dependence of  $R_H$  ( $\propto 1/T$ ) for the 2:2:2:3 phase samples. The carrier concentration  $n_H$  obtained for the sample, for which the highest  $T_c^{R=0}$  (107 K) is observed, is very close to that obtained by Rateau *et al.*<sup>10</sup> ( $1.7 \times 10^{21} \text{ cm}^{-3}$ ). However, this value of  $n_H$  is smaller than that reported by Oto *et al.*<sup>11</sup> for their single-phase sample ( $2.8 \times 10^{21} \text{ cm}^{-3}$ ). The strong temperature dependence of  $R_H$  for the 2:2:2:3 system is comparable with that for the 1:2:3 system.<sup>35</sup> One important difference between the 1:2:3 and 2:2:2:3 systems is that the temperature dependence of  $R_H$  (or  $n_H$ ) for the 2:2:2:3 system does not decrease appreciably with the suppression of transition temperature ( $T_c$ ). In the 1:2:3 system, the strong temperature dependence in  $R_H$  was assumed to originate from the two bands (1D chain and 2D planes).<sup>5</sup> This explanation is not applicable in the Bi systems. Thus, it appears that the temperature dependence of  $R_H$  and its suppression on doping in high- $T_c$  superconductors have some other common origin.

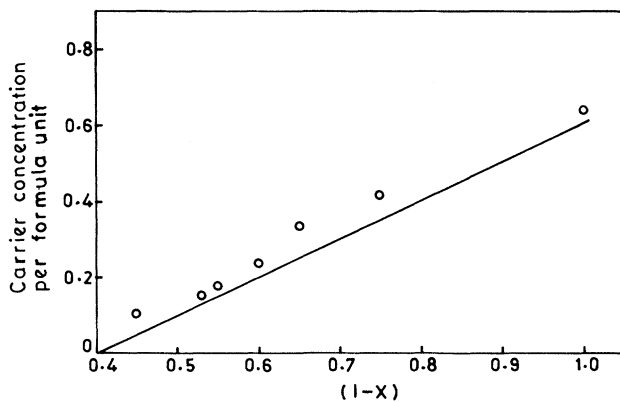


FIG. 8. The carrier concentration (per formula unit) at 120 K as a function of  $x$  for the  $\text{Bi}_2\text{Sr}_2\text{Ca}_{1-x}\text{Y}_x\text{Cu}_2\text{O}_{8+y}$  samples. The solid line is calculated, assuming that one Y atom substituted for a Ca atom removes one hole.

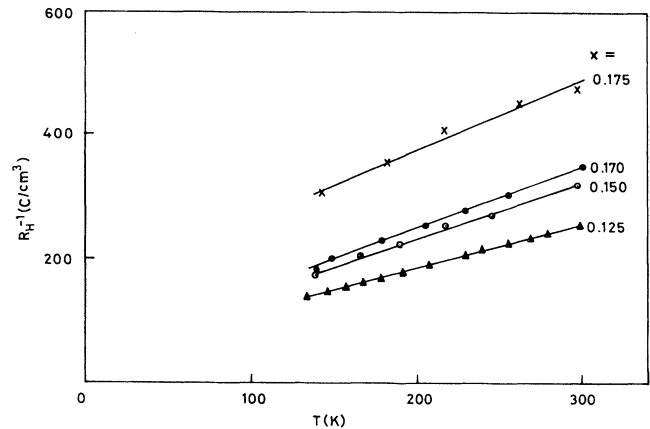


FIG. 9. The variation of the inverse Hall coefficient ( $R_H^{-1}$ ) as a function of temperature for the  $(\text{Bi}_{1-x}\text{Pb}_x)_2\text{Sr}_2\text{Ca}_2\text{Cu}_3\text{O}_{10+y}$  ( $x=0.125-0.175$ ) samples.

$T_c$  versus carrier concentration  $n_H$  is plotted in Figs. 10(a) and 10(b) for the Bi 2:2:1:2 and 2:2:2:3 systems, respectively. For the 2:2:1:2 system, superconductivity appears above a carrier concentration 0.07 holes/Cu.  $T_c$  increases with the increase of the carrier concentration, passes through a maximum at about  $n_H=3 \times 10^{21} \text{ cm}^{-3}$  (i.e., 0.32 hole/Cu atom) and then decreases with further

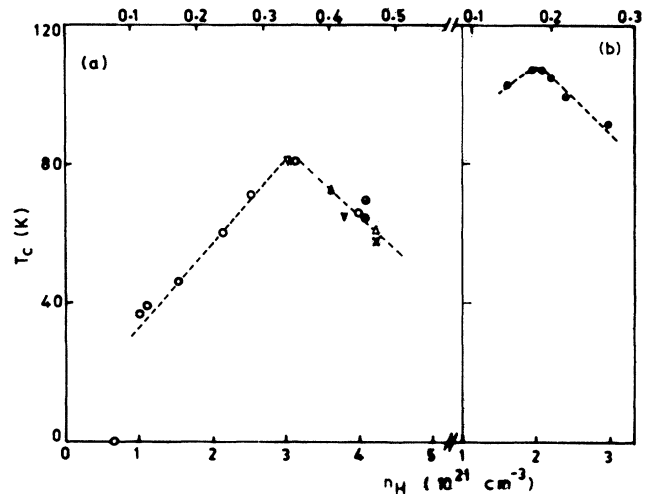


FIG. 10. (a) The correlation between  $T_c$  and  $n_H$  (at 300 K) in the Bi 2:2:1:2 system. The upper scale corresponds to the holes per Cu-ion.  $\circ$ :  $\text{Bi}_2\text{Sr}_2\text{Ca}_{1-x}\text{Y}_x\text{Cu}_2\text{O}_{8+y}$  (present work);  $\blacktriangle$ :  $(\text{Bi}_{0.75}\text{Pb}_{0.25})_2\text{Sr}_2\text{Ca}_2\text{Cu}_3\text{O}_{10+y}$  (Ref. 24);  $\blacktriangledown$ :  $(\text{Bi}_{0.70}\text{Pb}_{0.30})_2\text{Sr}_2\text{Ca}_2\text{Cu}_3\text{O}_{10+y}$  (present work);  $\times$ :  $(\text{Bi}_{0.875}\text{Ag}_{0.125})_2\text{Sr}_2\text{Ca}_2\text{Cu}_3\text{O}_{10+y}$  (present work);  $\nabla$ ,  $\circ$ , and  $\bullet$ :  $\text{BiSrCaCu}_2\text{O}_x$  (three samples prepared in three different methods) (Ref. 12, Mandal *et al.*). Although the nominal composition of some of the samples presented here is not 2:2:1:2, they contain a major amount of the 2:2:1:2 phase. (b) The correlation between  $T_c$  and  $n_H$  (at 300 K) in the  $(\text{Bi}_{1-x}\text{Pb}_x)_2\text{Sr}_2\text{Ca}_2\text{Cu}_3\text{O}_{10+y}$  system. The upper scale corresponds to the holes per Cu ion.

increase of the hole concentration. A similar variation of  $T_c$  versus  $n_H$  for Bi 2:2:2:3 has also been observed [Fig. 10(b)]. In this case, the maximum is observed at  $n_H = 2 \times 10^{21} \text{ cm}^{-3}$  (0.19 hole/Cu atom). Thus, for both the systems a correlation between the carrier concentration and superconductivity transition temperature exists. Similar dome-shaped curve has also been observed in the 2:1:4 and 1:2:3 systems.<sup>1</sup> In the 2:2:1:2 system, the carrier concentration for  $x = 0.25$  and 0 (sample *B*) is smaller than that of sample *A*, although the transition temperatures for the former samples are higher than the latter sample by 5 and 15 K, respectively. The results suggest that, as the hole concentration of the system increases above a critical value, the superconductivity is suppressed.

We now compare our results of Hall voltage measurements with those reported by other groups. The carrier concentration ( $n_H$ ) and transition temperature ( $T_c$ ) determined in the Y substituted samples are very close to the value reported by Tamegai *et al.*<sup>8</sup> Koike *et al.*<sup>9</sup> also measured  $n_H$  for a series of cation-substituted Bi 2:2:1:2 systems. In this case, Ca and Sr were substituted by Lu, Na and La, K, respectively. They observed the maximum in  $T_c$  at around 0.28 holes/Cu atom (for  $x = 0.2$ ) which is slightly smaller than our value. Allgeier and Schilling<sup>37</sup> studied the variation of  $T_c$  with oxygen content in the Bi 2:2:1:2 system and observed a  $T_c$  maximum at  $n_H \sim 0.32$ . In the  $\text{Bi}_4\text{Sr}_3\text{Ca}_{3-x}\text{Tm}_x\text{Cu}_4\text{O}_{16+y}$  system, Clayhold *et al.*<sup>31</sup> observed that  $n_H$  decreases linearly from 0.5 to 0.35 holes/Cu atom as  $x$  increases from 0 to 0.5, whereas  $T_c$  remains unaffected. Such a plateau in the  $T_c$  versus  $x$  (or  $n_H$ ) curve has not been observed by others including us. One common feature in the Bi 2:2:1:2 system is that when Ca-Sr is replaced by a small amount (20–30 %) of rare-earth elements,  $T_c$  is enhanced. Clayhold *et al.*<sup>31</sup> suggested that the high resistivity and low mobility  $\mu_H (=R_H/\rho)$  for their  $x = 0$  sample arises due to strong charge scattering by the modulation defects in the Bi-O planes. On Tm substitution, the strain due to modulation is reduced and leads to an improvement of  $\mu_H$  and  $T_c$ . However, the results of Koike *et al.*<sup>9</sup> and Tamegai *et al.*<sup>8</sup> show that both conductivity and mobility for the undoped system are large and  $T_c$  is low, which rules out the effect of any modulation suggested by Clayhold *et al.*<sup>31</sup> The suppression and disappearance of superconductivity in the heavily doped region is one of the characteristic features of all cuprate superconductors. In the  $\text{La}_{2-x}\text{Sr}_x\text{CuO}_4$  system, superconductivity disappears for  $x > 0.25$ , although the conductivity increases monotonically up to  $x = 0.34$  (Refs. 1 and 23). Similar behavior is observed in the  $\text{Tl}_2\text{Ba}_2\text{CuO}_6$  system also.<sup>3</sup> Samples annealed in an oxygen atmosphere do not show superconductivity even though the resistivity of these samples is small.  $T_c$  increases continuously up to 87 K with the decrease of oxygen content and, at the same time, both the conductivity and carrier density decreases. The correlation between  $T_c$  and  $n_H$  has also been established from muon-spin-relaxation ( $\mu\text{SR}$ ) and plasma frequency measurements. Uemura *et al.*<sup>13</sup> studied  $\mu\text{SR}$  for a series of high- $T_c$  samples with a different transition temperature.

They observed a universal linear relation between  $T_c$  and  $n_s/m^*$  for the four high- $T_c$  systems. They also found saturation and suppression of  $T_c$  in the heavily doped region. Saturation starts at different levels of  $n_s/m^*$  and progressively increases in systems 2:1:4, 1:2:3, 2:2:1:2, and 2:2:2:3. Similar behavior was observed from the optical reflectivity measurements by Tanaka.<sup>14</sup> They found that  $T_c$  increases linearly with  $\omega_p^2$  (the plasma frequency), which is proportional to  $n/m^*$ .

The above results are utilized to estimate several normal-state parameters, e.g., effective mass ( $m^*$ ) of the carriers, Fermi energy ( $E_F$ ), density of states [ $N(E_F)$ ], and the correlation energy ( $U$ ) due to on-site Coulomb repulsion. The plasma frequency of a system is related to  $n$  and  $m^*$  by the relation

$$\omega_p^2 = 4\pi n e^2 / m^* . \quad (6)$$

Using  $n = 2.0 \times 10^{21}$  (Ref. 6),  $3.5 \times 10^{21}$  (Ref. 35),  $3.0 \times 10^{21}$ , and  $1.5 \times 10^{21}$  per  $\text{cm}^3$ , we have calculated the effective masses as 4, 3, 3, and  $1 m_e$  for the 2:1:4, 1:2:3, 2:2:1:2, and 2:2:2:3 systems, respectively. (For the 2:2:2:3 system we have extrapolated the  $T_c$  versus  $\omega_p^2$  curve of Tanaka.<sup>14</sup>) The effective mass can also be calculated from the  $\mu\text{SR}$  experiment<sup>13</sup> and the values are obtained as 5, 4, 4, and  $1 m_e$  for the above systems, respectively. The effective mass calculated from the two different experiments agrees well with those reported from other measurements.<sup>38</sup>

The Fermi energy  $E_F [= \hbar^2(3\pi^2 n)^{2/3}/2m^*]$  and the Fermi velocity  $v_F [= (2E_F/m^*)^{1/2}]$  for the Bi 2:2:1:2 system may be computed using the above values of  $n$  and  $m^*$  ( $\sim 3m_e$ ). The Fermi energy and Fermi velocity for this system are 0.25 eV and  $1.7 \times 10^7$  cm/sec, respectively. These values are comparable with those of the La system<sup>38</sup> but much smaller than that of conventional metals ( $E_F = 5-10$  eV). Such a small value of  $E_F$  should lead to a significant decrease in the electronic contribution to the total heat capacity and thermal conductivity in the normal state. Thus, in these systems, the lattice contribution to the heat capacity and thermal conductivity will be large.

We now calculate the density of states at the Fermi level and this is given by

$$\begin{aligned} N(E_F) &= (1/2\pi^2)(2m^*/\hbar^2)^{3/2} E_F^{1/2} \\ &= 1.8 \times 10^{22} \text{ state/eV cm}^3 \\ &\sim 1 \text{ states/eV Cu spin} . \end{aligned} \quad (7)$$

This value of density of states may be compared with that obtained from the specific-heat jump at the transition temperature. Fisher *et al.*<sup>29</sup> measured specific heat in the Bi 2:2:1:2 system and obtained a  $\gamma$  value of  $11 \text{ mJ mol}^{-1} \text{ K}^{-2}$  which corresponds to 1.1 states/eV Cu spin. Okazaki *et al.*<sup>30</sup> measured the specific heat for the Pb-doped 2:2:2:3 phase Bi sample and obtained a slightly smaller value of  $N(E_F) = 0.8 \text{ state/eV Cu spin}$ .

The Pauli paramagnetic susceptibility  $\chi_p$  is given by

$$\chi_p = \mu_B^2 N(E_F) , \quad (8)$$



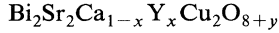
where  $N(E_F)$  is the density of states in the presence of electron-electron correlation and is given by

$$N(E_F) = \frac{N_0(E_F)}{1 - UN_0(E_F)/2}, \quad (9)$$

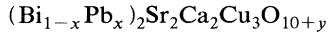
where  $N_0(E_F)$  is the free-electron density of states. Using  $\chi_p = 5.7 \times 10^{-4}$  emu/mol for the  $x=0$  sample (Sec. IV C),  $N(E_F)$  is obtained as 4.4 states/eV Cu spin, which gives the value of the Coulomb correlation energy  $U \sim 5.5$  eV. This value of  $U$  is comparable to that obtained in the 1:2:3 system (5 eV) by Cheong *et al.*<sup>39</sup> The density of states calculated from the observed magnetic susceptibility is about four times larger than the value obtained from the specific-heat measurement. A similar discrepancy has also been observed in the 1:2:3 system.<sup>39</sup>

## V. CONCLUSION

We have prepared a number of



and



samples with varying  $x$  and performed x-ray, electrical resistivity, magnetic susceptibility, and Hall measurements on these samples. The lattice parameter  $c$  in  $\text{Bi}_2\text{Sr}_2\text{Ca}_{1-x}\text{Y}_x\text{Cu}_2\text{O}_{8+y}$  samples decreases with doping concentration ( $x$ ) which is attributed to the smaller size of the dopant ( $\text{Y}^{3+}$  ion). The  $a$  parameter, on the other hand, increases with  $x$  which is believed to be due to the increase in the Cu—O bond length with the decrease of carrier concentration. The normal-state resistivity of the

$\text{Bi}_2\text{Sr}_2\text{Ca}_{1-x}\text{Y}_x\text{Cu}_2\text{O}_{8+y}$  samples shows that the system undergoes a metal-to-semiconductor transition at  $x=0.55$ . For the  $x > 0.55$  samples, the conduction follows a 2D VRH mechanism, whereas for  $x=0.55$ , it is 3D VRH in nature. The localization length  $\alpha^{-1}$  has been calculated for various concentrations which, as expected, increase as the system approaches the metallic region. In the high-temperature region, the resistivity arises due to the phonon-assisted hopping of small polarons. From the magnetic susceptibility measurement in the  $\text{Bi}_2\text{Sr}_2\text{Ca}_{1-x}\text{Y}_x\text{Cu}_2\text{O}_{8+y}$  samples, the Pauli susceptibility is calculated to be in the range  $(5.7-3.7) \times 10^{-4}$  emu/mol.  $R_H^{-1}$  is positive and has a linear temperature dependence.  $R_H^{-1}$  is proportional to the doping concentration ( $x$ ), the behavior predicted for a strongly correlated Hubbard system. The temperature dependence of  $R_H$  is stronger in the 2:2:2:3 phase compared to the 2:2:1:2 phase. The  $T_c$  versus  $n_H$  curve is dome-shaped; the superconductivity appears above a critical concentration (0.07 holes/Cu for the 2:2:1:2 system), increases linearly with  $n_H$  until a maximum is reached, and then decreases with further increase of carrier concentration. Several normal-state parameters like the effective mass of the carrier, Fermi energy, density of states, correlation energy ( $U$ ), etc., have been calculated and compared to those reported in the literature. A large value of the effective mass ( $1-5 m_e$ ) and low Fermi energy are the characteristics of the high- $T_c$  superconductors.

## ACKNOWLEDGMENTS

The authors are grateful to Dr. A. N. Das for many helpful discussions and S. N. Datta and A. Pal for technical help.

- <sup>1</sup>J. B. Torrance, A. Bezing, A. I. Nazzal, and S. S. P. Parkin, *Physica C* **162-164**, 291 (1989); J. M. Tranquada, A. H. Moudden, A. I. Goldman, P. Zolliker, D. E. Cox, G. Shirane, S. K. Sinha, D. Vaknin, D. C. Johnston, M. S. Alvarez, and A. J. Jacobson, *Phys. Rev. B* **38**, 2477 (1988).
- <sup>2</sup>J. B. Torrance, Y. Tokura, A. I. Nazzal, A. Bezing, T. C. Huang, and S. S. P. Parkin, *Phys. Rev. Lett.* **61**, 1127 (1988).
- <sup>3</sup>Y. Shimakawa, Y. Kubo, T. Manako, and H. Igarashi, *Phys. Rev. B* **40**, 11 400 (1989).
- <sup>4</sup>A. Matsuda, K. Kinoshita, T. Ishii, H. Shibata, T. Watanabe, and T. Yamada, *Phys. Rev. B* **38**, 2910 (1988).
- <sup>5</sup>Z. Z. Wang, J. Clayhold, N. P. Ong, J. M. Tarascon, L. H. Greene, W. R. McKinnon, and G. W. Hull, *Phys. Rev. B* **36**, 7222 (1987).
- <sup>6</sup>N. P. Ong, in *Physical Properties of High-Temperature Superconductors II*, edited by D. M. Ginsberg (World-Scientific, Singapore, 1990), and references therein.
- <sup>7</sup>H. Takagi, T. Ido, S. Ishibashi, M. Uota, and S. Uchida, *Phys. Rev. B* **40**, 2254 (1989).
- <sup>8</sup>T. Tamegai, K. Koga, K. Suzuki, M. Ichihara, F. Sakai, and Y. Iye, *Jpn. J. Appl. Phys.* **28**, L112 (1989).
- <sup>9</sup>Y. Koike, Y. Iwabuchi, S. Hosoya, N. Kobayashi, and T. Fukase, *Physica C* **159**, 105 (1989).
- <sup>10</sup>M. Rateau, R. Suryanarayanan, O. Gorochoy, and H. Panikowska, *Phys. Rev. B* **41**, 857 (1990).
- <sup>11</sup>K. Oto, K. Murase, and S. Takaoka, *Solid State Commun.* **71**, 819 (1989).
- <sup>12</sup>P. Mandal, A. Poddar, A. N. Das, B. Ghosh, and P. Choudhury, *Phys. Rev. B* **40**, 730 (1989); J. Clayhold, N. P. Ong, P. H. Hor, and C. W. Chu, *ibid.* **38**, 7016 (1988).
- <sup>13</sup>Y. J. Uemura, G. M. Luke, B. J. Sternlieb, J. H. Brewer, J. F. Carolan, W. N. Hardy, R. Kadono, J. R. Kempton, R. F. Kiefl, S. R. Kreitzman, P. Mulhern, T. M. Riseman, D. L. Williams, B. X. Yang, S. Uchida, H. Takagi, J. Gopalakrishnan, A. W. Sleight, M. A. Subramanian, C. L. Chien, M. Z. Cieplak, G. Xiao, V. Y. Lee, B. W. Statt, C. E. Stronach, W. J. Kossler, and X. H. Yu, *Phys. Rev. Lett.* **62**, 2317 (1989).
- <sup>14</sup>S. Tanaka, *Phys. Scr. T27*, 7 (1989), and references therein.
- <sup>15</sup>R. J. Birgeneau, C. Y. Chen, D. R. Gabbe, H. P. Jenssen, M. A. Kastner, C. J. Peters, P. J. Picone, T. Thio, T. R. Thurston, H. L. Tuller, J. D. Axe, P. Böni, and G. Shirane, *Phys. Rev. Lett.* **59**, 1329 (1987); N. W. Preyer, R. J. Birgeneau, C. Y. Chen, D. R. Gabbe, H. P. Jenssen, M. A. Kastner, P. J. Picone, and T. Thio, *Phys. Rev. B* **39**, 11 563 (1989); C. Uher and A. B. Kaiser, *ibid.* **37**, 127 (1988); E. J. Osquiguil, L. Civale, R. Decca, and F. de la Cruz, *ibid.* **38**, 2840 (1988); S.-W. Cheong, Z. Fisk, R. S. Kwok, J. P. Remeika, J. D. Thompson, and G. Gruner, *ibid.* **37**, 5916 (1988).
- <sup>16</sup>B. Ellman, H. M. Jaeger, D. P. Katz, T. F. Rosenbaum, A. S. Cooper, and G. P. Espinosa, *Phys. Rev. B* **39**, 9012 (1989).
- <sup>17</sup>N. F. Mott, *Metal Insulator Transitions* (Taylor and Francis, London, 1974), and references therein; I. G. Austin and N. F.

- Mott, *Adv. Phys.* **18**, 41 (1969).
- <sup>18</sup>R. S. Kwok, S.-W. Cheong, J. D. Thompson, Z. Fisk, J. L. Smith, and J. O. Willis, *Physica C* **152**, 240 (1988).
- <sup>19</sup>R. Yoshizaki, Y. Saito, Y. Abe, and H. Ikeda, *Physica C* **152**, 408 (1988).
- <sup>20</sup>H. Fukuyama and Y. Hasegawa, *Physica B&C* **148**, 204 (1987); A. N. Das, B. Ghosh, and P. Choudhury, *Physica C* **158**, 311 (1989).
- <sup>21</sup>S. Martin, A. T. Fiory, R. M. Fleming, L. F. Schneemeyer, and J. V. Waszczak, *Phys. Rev. B* **41**, 846 (1990), and references therein; R. A. Fisher, S. Kim, Y. Wu, N. E. Phillips, H. M. Ledbetter, and K. Togano, *Physica C* **162-164**, 502 (1989).
- <sup>22</sup>For example, see J. J. Lin, E. L. Benitez, S. J. Poon, M. A. Subramanian, J. Gopalakrishnan, and A. W. Sleight, *Phys. Rev. B* **38**, 5095 (1988).
- <sup>23</sup>K. Sreedhar and P. Ganguly, *Phys. Rev. B* **41**, 371 (1990).
- <sup>24</sup>A. Poddar, P. Mandal, A. N. Das, B. Ghosh, and P. Choudhury, *Physica C* **161**, 567 (1989).
- <sup>25</sup>The term insulator here refers to a nonmetallic state where the electrical resistivity increases with decreasing temperature, similar to semiconducting behavior.
- <sup>26</sup>N. F. Mott, *J. Non-Cryst. Solids* **1**, 1 (1969).
- <sup>27</sup>The difference between the  $n = \frac{1}{3}$  and  $\frac{1}{4}$  fittings for the  $x = 0.55$  sample is negligible, the standard deviation in the resistance being  $1.720 \times 10^{-3}$  for the  $n = \frac{1}{3}$  and  $1.699 \times 10^{-3}$  for the  $n = \frac{1}{4}$  fittings. The temperature range, for which the fitting is valid, is small for this sample, compared to others. The deviation from the exponential curve for the  $x = 0.55$  sample in the low temperatures occurs presumably due to the formation of superconducting islands. Similar behavior has been observed by Yoshizaki *et al.* (Ref. 19).
- <sup>28</sup>W. Brenig, G. H. Döhler, and H. Heyszenau, *Philos. Mag.* **27**, 1093 (1973).
- <sup>29</sup>R. A. Fisher, S. Kim, S. E. Lacy, N. E. Phillips, D. E. Morris, A. G. Markelz, J. Y. T. Wei, and D. S. Ginley, *Phys. Rev. B* **38**, 11 942 (1988).
- <sup>30</sup>N. Okazaki, T. Hasegawa, K. Kishio, K. Kitazawa, A. Kishi, Y. Ikeda, M. Takano, K. Oda, H. Kitaguchi, J. Takada, and Y. Miura, *Phys. Rev. B* **41**, 4296 (1990).
- <sup>31</sup>J. Clayhold, S. J. Hagen, N. P. Ong, J. M. Tarascon, and P. Barboux, *Phys. Rev. B* **39**, 7320 (1989).
- <sup>32</sup>C. M. Foster, A. J. Heeger, Y. H. Kim, and G. Stucky, *Synth. Met.* **33**, 171 (1989); C. Taliani, R. Zamboni, G. Ruani, F. C. Matocotta, and K. I. Pokhodnya, *Solid State Commun.* **66**, 487 (1988); C. M. Foster, A. J. Heeger, G. Stucky, and N. Herron, *ibid.* **71**, 945 (1989); D. Mihailovic, C. M. Foster, K. Voss, and A. J. Heeger, *Phys. Rev. B* **42**, 7989 (1990).
- <sup>33</sup>V. V. Moshchalkov, *Physica C* **156**, 473 (1988); F. Devaux, A. Manthiran, and J. B. Goodenough, *Phys. Rev. B* **41**, 8723 (1990).
- <sup>34</sup>D. C. Johnston, S. K. Sinha, A. J. Jacobson, and J. M. Newsam, *Physica C* **153-155**, 572 (1988).
- <sup>35</sup>T. Penney, S. von Molnar, D. Kaiser, F. Holtzberg, and A. W. Kleinsasser, *Phys. Rev. B* **38**, 2918 (1988).
- <sup>36</sup>H. Takagi, H. Eisaki, S. Uchida, A. Maeda, S. Tajima, K. Uchinokura, and S. Tanaka, *Nature* **332**, 236 (1988); G. Brinceno and A. Zettl, *Phys. Rev. B* **40**, 11 352 (1989).
- <sup>37</sup>C. Allgeier and J. S. Schilling, *Physica C* **168**, 499 (1990).
- <sup>38</sup>V. Z. Kresin and S. A. Wolf, *Phys. Rev. B* **41**, 4278 (1990), and references therein.
- <sup>39</sup>S.-W. Cheong, S. E. Brown, Z. Fisk, R. S. Kwok, J. D. Thompson, E. Zirngiebl, G. Gruner, D. E. Peterson, G. L. Wells, R. B. Schwarz, and J. R. Cooper, *Phys. Rev. B* **36**, 3913 (1987).